

# A Non-invasive Blood Glucose Monitoring System Based on Smartphone PPG Signal Processing and Machine Learning

Gaobo Zhang, Zhen Mei, Yuan Zhang\*, Senior Member, IEEE, Xuesheng Ma, Benny Lo, Senior Member, IEEE, Dongyi Chen, and Yuanting Zhang, Fellow, IEEE

**Abstract**—Blood glucose level needs to be monitored regularly for managing the health condition of hyperglycemic patients. The current glucose measurement approaches still rely on invasive techniques which are uncomfortable and raise the risk of infection. To facilitate daily care at home, we propose an intelligent, non-invasive blood glucose monitoring system which can differentiate a user's blood glucose level into normal, borderline and warning based on smartphone PPG signals. The main implementation processes of the proposed system include: (1) a novel algorithm for acquiring photoplethysmography (PPG) signals using only smartphone camera videos; (2) a fitting-based sliding window (FSW) algorithm to remove varying degrees of baseline drifts and segment the signal into single periods; (3) extracting characteristic features from the Gaussian functions by comparing PPG signals at different blood glucose levels; (4) categorizing the valid samples into three glucose levels by applying machine learning algorithms. Our proposed system was evaluated on a data set of 80 subjects. Experimental results demonstrate that the system can separate valid signals from invalid ones at an accuracy of 97.54% and the overall accuracy of estimating the blood glucose levels reaches 81.49%. The proposed system provides a reference for the introduction of non-invasive blood glucose technology into daily or clinical applications. This research also indicates that smartphone-based PPG signals have great potential to assess an individual's blood glucose level.

**Index Terms**—Non-invasive Blood Glucose Monitoring, Smart-

This work was supported in part by the National Natural Science Foundation of China under Grant 61572231 and 61572110, and in part by the Newton Fund Researcher Links Workshop under Grant 2017-RLWK9-11046. (*Equal Contribution: Gaobo Zhang and Zhen Mei; Corresponding Author: Yuan Zhang.*)

Gaobo Zhang is with Chongqing Key Laboratory of Nonlinear Circuits and Intelligent Information Processing, College of Electronic and Information Engineering, Southwest University, Chongqing 400715, China, and also with the Shandong Provincial Key Laboratory of Network Based Intelligent Computing, University of Jinan, Jinan 250022, China (e-mail: gaoboz0906@gmail.com).

Zhen Mei is with the College of Chemistry and Chemical Engineering, Southwest University, Chongqing 400715, China (e-mail: meizhen1122@163.com).

Yuan Zhang is with the Chongqing Key Laboratory of Nonlinear Circuits and Intelligent Information Processing, College of Electronic and Information Engineering, Southwest University, Chongqing 400715, China (e-mail: yuanzhang@swu.edu.cn).

Xuesheng Ma is with the School of Natural Medicine, University of the Western Cape, Cape Town BNT 371, South Africa (e-mail: xma@uwc.ac.za).

Benny Lo is with the Hamlyn Centre and the Department of Surgery and Cancer, Imperial College London, London, SW7 2AZ, U.K. (e-mail: benny.lo@imperial.ac.uk).

Dongyi Chen is with the School of Automation Engineering, University of Electronic Science and Technology of China, Chengdu 611731, China (e-mail: chenxigt@hotmail.com).

Yuanting Zhang is with the Department of Mechanical and Biomedical Engineering, City University of Hong Kong, Hong Kong 999077, China (e-mail: yt.zhang@cityu.edu.hk).

phone PPG Signal, Gaussian Fitting, Healthcare based on Machine Learning, Daily Care.

## I. INTRODUCTION

**D**IABETES is a lifelong metabolic disease characterized by chronic hyperglycemia due to multiple causes such as impaired insulin secretion and impaired biological effects [1]. Currently, there is no effective treatment of diabetes, but regular monitoring of blood glucose level can reduce or delay the incidence of complications [2]. Self-monitoring is considered as one of the most direct and feasible options for controlling diabetes [3].

The mature detection technique is to use a blood glucose analyzer to measure the glucose level of a blood sample obtained by piercing the top of the patient's finger. This method does not only cause pain and burden to the patients due to frequent blood collection, but also does not allow real-time monitoring [4], [5]. Non-invasive blood glucose technology can overcome the above shortcomings and has become a popular topic in smart healthcare research [6]. However, non-invasive blood glucose monitoring system for self-monitoring is still in the early stage of development and far from ready to be deployed for home care.

Photoplethysmography (PPG) technique has been applied to measure blood volume changes in certain parts of the body [7], [8]. A PPG device usually consists of a light source for illuminating the tissue, and a detector for sensing the reflected light, respectively. The amount of light absorbed varies periodically according to fluctuations of blood volume in the circulatory system, so that the PPG signals contain information related to breathing, circulatory system, blood flow and heartbeat [9], [10]. Nabeel [11] proposed a non-invasive blood pressure measurement, and Motin [12] performed effective heart rate and respiratory rate monitoring. Both works are accomplished by analyzing specific components in the PPG signals. Processing PPG signal can reveal new information on the body's hemodynamic characteristics and certain blood parameters, which are of great significance for personal health monitoring [13].

At present, most of the human physiological measurements using photoelectric information are rely on professional acquisition equipments. In [14], PPG signals from normal and hyperglycemic patients were obtained using a Glutrac connected to cloud processing system. Although this method

can obtain high quality data, it has certain cost limitations and difficulties to be used ubiquitously. Therefore, we aim to obtain PPG signals through the use of the smartphone camera to capture and then analyzing the variation of light intensity reflected from a finger caused by the change of blood volume in systolic and diastolic cycles.

Recent breakthrough in artificial intelligence and medical fields has been widely applied for clinical decision support and medical image processing. Our proposed system utilizes machine learning algorithms to estimate blood glucose levels via PPG signals retrieved from smartphone. Our main contributions include:

- A few methods for PPG signal retrieval have been developed in literature, however most of them rely on professional equipments. We propose a novel algorithm to extract PPG signals from only smartphone video. Experimental results indicate that our algorithm is effective for extracting PPG signals which are extremely weak and susceptible to noise interference. Consequently, our method fits well with home self-monitoring due to its portability and ease of use.
- Traditional approaches usually removed baseline drift through high-pass filtering. Considering the fact that signal components are complex and there exist varying degrees of baseline drift, we develop a fitting-based sliding (FSW) algorithm to remove baseline drift meanwhile dividing the signals into single periods. Therefore, the original characteristics of the PPG signals are retained to a great extent, meanwhile distortion introduced by filtering is avoided.
- We propose a feature extraction method based on Gaussian fitting to find out the correspondence between the hyperglycemia and the normal human PPG signals in both time domain and frequency domain by analyzing the parameters of the positive Gaussian function. Experimental results suggest that features extracted by this method can efficaciously divide blood glucose into three levels (normal, borderline and warning).

The rest of the paper is organized as follows. Section II presents the related work. Section III describes the proposed methodology in detail. Results obtained by experiment are explained in section IV and section V concludes the paper.

## II. RELATED WORK

Non-invasively tracking blood glucose levels is now possible due to various breakthroughs in optics and electrochemistry. We focus on the work related to measuring blood glucose based on PPG signals and summarize the representative researches as follows.

In [1], PPG reflecting the heart cycle was acquired according to different optical intensity through the self-made embedded finger clip, composed of LED and photodiode. It bases on the hypothesis that the transmittance of light is inversely proportional to the blood glucose concentration. The acquired signal was converted into the digital signal by combining high-pass filter, amplifier and fourth-order low-pass filter to eliminate the high frequency noise. The motion artifacts were then

processed using an adaptive adaline neural network filter. The invasive blood glucose meter was used to label the subject's actual blood glucose level, which is then combined with the filtered PPG signal to predict blood glucose levels using an artificial neural network integrated into a field programmable gate array (FPGA). The data were from 50 individuals with different blood glucose levels, and the estimated accuracy was 95.38%. Light conditions and adipose tissue can affect system performance. The acquisition of the signal was simple and portable, but the processing was complicated, and it could not offer the advantage of real-time monitoring.

Tsai [14] used a wearable health device called Glutrac to obtain PPG signals from fingers and wrists, and then sent the acquired signals to NoSQL databases via Bluetooth 5.0 for cloud storage and calculation. After signal denoising, 30 features were extracted from the time domain and its first derivative. In the experiment, multiple decision trees were used for data learning. Nine patients with type 2 diabetes participated in the trial and invasive blood glucose values were obtained by finger puncture using Accuc-chek. The global accuracy of the model reached 80%, however the accuracy varied greatly between different individuals.

Monte-Moreno [15] proposed the use of respiratory frequency, heart rate, vascular compliance, blood viscosity and other physiological parameters to analyze the PPG waveform and then estimate blood glucose. After acquiring the PPG by the finger clip, denoising was performed to remove motion artifacts for feature extraction. Finally, among support vector machine (SVM), random forest, linear regression and neural network classifiers, random forest performed better than other classifiers. Using Clark Grid Analysis (CGA), 87.7% of the points fell into Zone A. Hina [16] presented a non-invasive glucose monitoring prototype system composing of three main modules. The first module, consisting of a clip and a LED, was implemented on a printed circuit board (PCB) to obtain PPG signals. The second module performed signal preprocessing whereafter 10 features were extracted on the FPGA. The third module used a machine learning index Gaussian process regression (GPR) model to measure blood glucose levels. Data were collected from 200 volunteers including 4 diabetic patients. The mean absolute relative difference (mARD) in predicted blood glucose levels was 8.97%. The acquired signal was also transmitted to a computer for further processing, which is time consuming. Rachim [17] collected PPG signals under different optical wavelengths by wearable biosensors. Digital wavelet transform (DWT) and wavelet decomposition (WD) were used to remove the baseline wander of the original PPG signals. After applying the local maxima algorithm for signal peak detection, 24 features were extracted from each periodic PPG signal. The model was based on a linear partial least squares (PLS) multivariate calibration and was evaluated by 10-fold cross validation. A total of 12 subjects participated in the experiment. The standard error of prediction (SEP) and the correlation coefficient ( $R_p$ ) between the estimated and the reference blood glucose were 6.16 mg/dL and 0.86, respectively. The above three methods require individual-based calibration and can not work in multi-user scenarios.

To sum up, there is up to now no non-invasive blood glucose

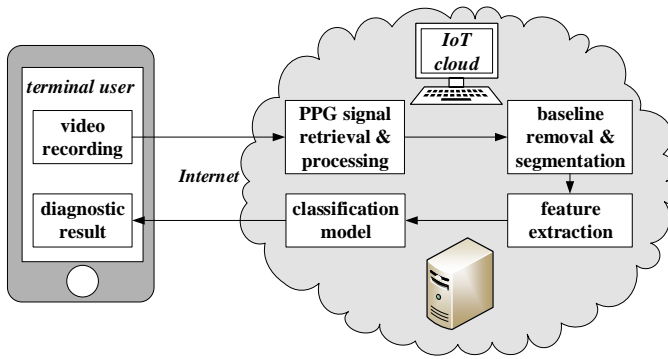


Fig. 1. Smartphone PPG based non-invasive blood glucose monitoring system.

monitoring system based on PPG signals from smartphone, which has the advantages of portability, time efficiency and no calibration requirement.

### III. PROPOSED SYSTEM

Users can record video and acquire blood glucose level through a smartphone. Signal retrieval and preprocessing are performed in the cloud, and the final result is obtained after feature extraction and classification. Fig. 1 shows the proposed system functional flowchart. Blood glucose scale is divided into 3 groups ranging from 3.9 mmol/L to 11 mmol/L, and the corresponding levels are also listed in the table I.

TABLE I  
BLOOD GLUCOSE GROUPS.

Groups	Blood Glucose Ranges (mmol/L)	Level
G1	3.9-6.1	Normal
G2	6.2-7.8	Borderline
G3	7.9-11	Warning

#### A. Smartphone Video Recording

A 60-second video of the left index finger was recorded using a 30-frame-rate (sampling rate 30 Hz) iPhone 6s Plus camera. Fingertip must cover both the flash and the camera simultaneously. Light and dark switched obviously in the video as the finger's blood volume varies, whereafter an invasive ACCU-CHEK Advantage blood glucose meter complying with the international standard ISO15197 (2013) was used to detect the actual blood glucose value for labeling (3 groups). These two procedures were performed consecutively but separately (the interval was less than one minute), so that the blood glucose level did not fluctuate in such a short time. The video was then transferred to a computer for further processing with MATLAB.

The quality of the video recording is subject to the position of fingertip on the camera, the pressure of fingertip and the lighting conditions [18]. Therefore, a usability evaluation scheme for the smartphone video is proposed to monitor the saturation of each color channel in the frame. Chromatic parameters including average value of the red Ave(R), green Ave(G) and blue Ave(B) channels, as well as the corresponding standard deviation of the red channel  $\sigma_R$ , are evaluated frame

by frame. We implemented a statistical analysis of each chrominance parameter to provide a suitable threshold. A total of 3000 video frames from the first 5 seconds of 20 subjects under correct operations were used to calculate and select the critical value of the distribution range of each parameter as the threshold.

Table II summarizes the conditions for proper video recording. If the chromatic parameters in a certain frame do not meet the above conditions, it means that video has not been properly recorded. It should be noted that the evaluation of the video usability is only for preliminary screening to ensure a user's correct operation so that PPG signals could be extracted. The removal of the unavoidable baseline drift is described in subsection III.C.

TABLE II  
CONDITIONS FOR EVALUATING VIDEO USABILITY.

$\text{Ave}(R) \geq 240$
$\sigma_R \leq 20$
$\text{Ave}(G) < 1$
$\text{Ave}(B) < 75$

Table III presents four frames among which the first two frames are recognized to be operationally correct and can be accepted for further analysis. Chrominance parameters of the last two frames do not meet the requirements specified, hence are discarded.

TABLE III  
EXAMPLE OF EVALUATING VIDEO USABILITY.

Frame	Chromatic parameters	Note
	$\text{Ave}(R)=244.11$ $\sigma(R)=15.76$ $\text{Ave}(G)=0.23$ $\text{Ave}(B)=32.37$	Acceptable
	$\text{Ave}(R)=245.37$ $\sigma(R)=19.17$ $\text{Ave}(G)=0.15$ $\text{Ave}(B)=70.33$	Acceptable
	$\text{Ave}(R)=254.22$ $\sigma(R)=1.33$ $\text{Ave}(G)=22.20$ $\text{Ave}(B)=127.87$	Not Acceptable
	$\text{Ave}(R)=123.03$ $\sigma(R)=82.28$ $\text{Ave}(G)=113.16$ $\text{Ave}(B)=99.93$	Not Acceptable

#### B. PPG Signal Retrieval

The absorption of light by blood is associated with the change of finger blood volume, which is reflected and recorded in the video. Accordingly, the pixel intensity of the same area in adjacent frames is different. We calculate a continuous PPG

signal based on the overall changes of pixel intensity in each video frame. The red, green and blue channels are separated from a single frame of the correctly recorded video, as shown in Fig. 2(a) and 2(b). A threshold is set for each frame using Eq. (1), and the PPG value of frame  $i$  is calculated by Eq. (2) which is the sum of the pixels with intensity greater than a specified threshold. PPG signal is then obtained by plotting the calculated sums of each frame pixel.

$$\text{Threshold} = 1.01 \times (\text{intensity}_{\max} - \text{intensity}_{\min}) \quad (1)$$

$$\text{PPG}_{\text{signal}}[i] = \sum_{1}^{\text{total pixels}} \text{intensity} > \text{Threshold} \quad (2)$$

The threshold is selected empirically. When threshold gets lower and the output becomes smoother, signal eventually turns into a horizontal line. If threshold keeps getting higher, the signal will gradually reach some peaks, which will affect the signal quality. Taking full consideration of the waveform accuracy and without loss of generality, threshold in our proposed system is defined as 1.01 times of the pixel intensity range.

To determine the channel that can generate PPG signals after a simple calculation, the signals are extracted from all three channels (red, green, blue) as shown in Fig. 2(c). It is evident that PPG signals obtained from the red channel are the clearest and do not require further processing to reflect the periodic variation of blood volume during cardiac cycles. While green and blue channels are difficult to extract useful information without other complicated processing.

### C. Raw PPG Signal Preprocessing

When the light cast on the skin, it will be detected by the photodiode in two modes: transmission mode where the light penetrates through the skin and tissue of a finger or ear lobe and is detected by the photo-detector on the other side, and reflection mode where the light is shinned onto the skin and reflected and picked up by a photo-detector positioned next to the light source [19]. In our scenario, the smartphone's flash lights up the finger (its tissue, bones and blood vessels) and the reflected light is captured by the camera on the same side of the finger. Therefore, the original PPG signals retrieved from the recorded video are reversed and need to be inverted to recover to normal case as shown in Fig. 3(a) and 3(b), respectively. Reflective mode PPG signals are susceptible to noise such as ambient light, temperature, power frequency interference so that the inverted signals are denoised by a six-order Butterworth filter to remove the frequency components higher than 16 Hz after Fourier analysis, as shown in Fig. 3(c).

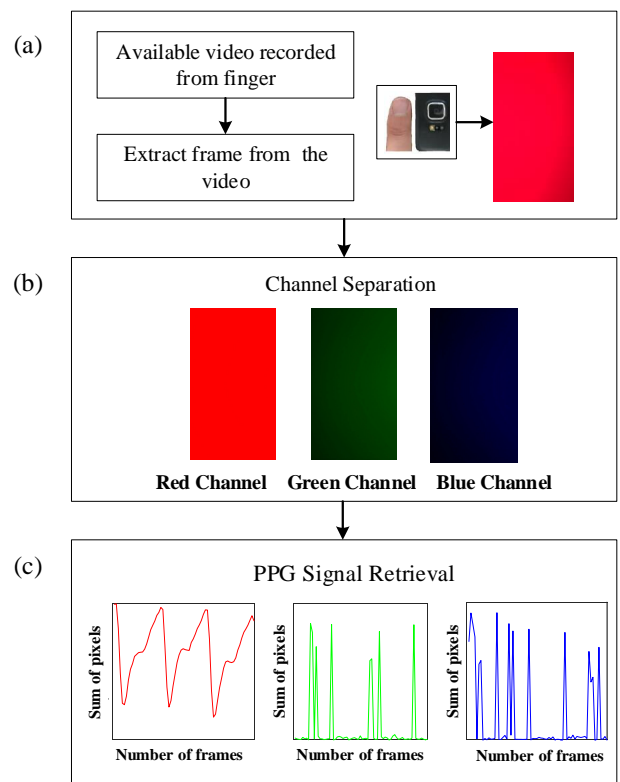


Fig. 2. PPG signal retrieval methodology. (a) video recording using smartphone camera and a sample frame extracted from the video, (b) red, green and blue components of a frame, (c) PPG signals retrieved from the red, green and blue components, respectively.

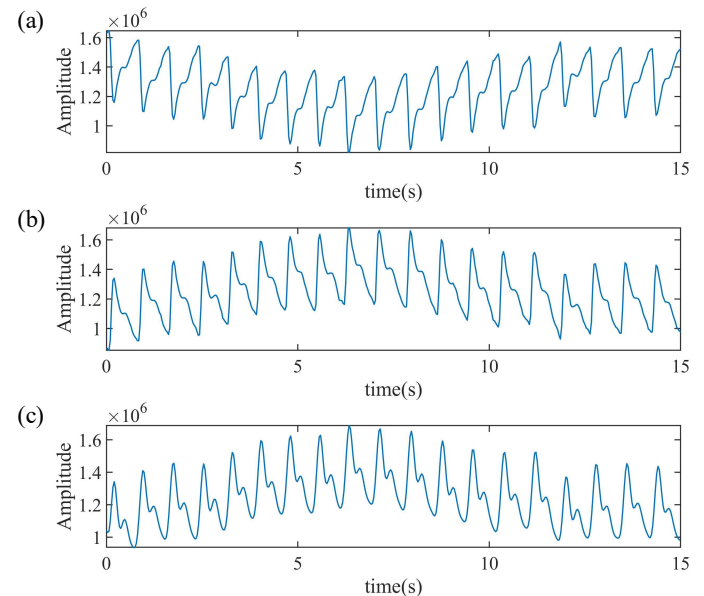


Fig. 3. Signal preprocessing stage. (a) Raw smartphone PPG signal, (b) Inverted smartphone PPG signal, (c) Filtered smartphone PPG signal.

During the video capture, the smartphone camera is simply attached to the fingertip, which could easily introduce motion artifacts to the extracted PPG signals. Although this does not lead to significant baseline drifts, the inherent waveform characteristics of the raw single-period signals will be distorted. Removing low-frequency components to get rid of the baseline

drifts will result in the loss of some useful information in the waveform. Therefore, the details should be better preserved to ensure that the pathological features of the signal are not lost.

Sliding window algorithm is widely adopted for trending and rhythm analysis of continuous dynamic physiological signals to explore pathological information. In [20], feature extraction and heart rate calculation of PPG signals were performed using sliding window algorithm. In [21], sliding window was used to find peaks and valleys. However, due to the existence of baseline drift, the valleys were not well recognized. Once the valley was identified incorrectly, the probability of the next valley being wrong became higher. Therefore the valleys should be identified as accurately as possible. Consequently, we propose FSW algorithm to remove baseline drift, after that signal is brought back to its normal base (x-axis) and segmented into single periods. The valleys of the PPG signal are accurately recognized using a sliding window and through an automatic error correction mechanism. The cubic spline is utilized to fit the baseline of the signal with these valleys.

#### Algorithm 1 Fitting-based sliding window (FSW).

**Input:** Clean smartphone PPG signal, *signal*;  
**Output:** single-period samples after baseline remove, *signal<sub>i</sub>*;

- 1: Get main frequency, *f*;
- 2: Set a window size =  $0.7 * 1/f$ ;
- 3: Slide the window to find minimum of each window, The values of these local minimums and its corresponding index are recorded as *y* and *x*.
- 4: Utilize cubic spline function to fit baseline with *x* and *y*, and save the values in the array *baseline*;
- 5: Separate the point in the signal that matches *baseline*-*signal*>0, find the smallest amplitude *m*, and then replace *x* and *y* in the current *baseline*;
- 6: Start with the current signal value, iterate steps 2 – 5 and update *x* and corresponding *y* values in the *baseline*;
- 7: *signal*-*baseline*;
- 8: Segment *n* into *n<sub>i</sub>* according to *x*;
- 9: **return** *n<sub>i</sub>*;

The pseudocode in Algorithm 1 provides the entire process of the FSW algorithm. For the purpose of periodic segmentation, correctly localizing all the valleys of the continuous PPG signals is a key prerequisite. Through extensive experiments, we set the window size to be 7/10 period, among all the possibilities, to realize good performance in terms of accuracy and real time response. The period length is obtained by analyzing the frequency of the periodic signal. One advantage of FSW algorithm lies in its automatic correction of those valleys mistakenly identified. Once the baseline is noticed to be greater than the signal, the minimum value of the segmented signal will be adopted as the new valley from which the window will be re-established to update the subsequent valley value. In this case the loop body ends when no baseline is greater than the signal. Fig. 4(a) indicates that FSW algorithm performs well in identifying valleys of the continuous PPG

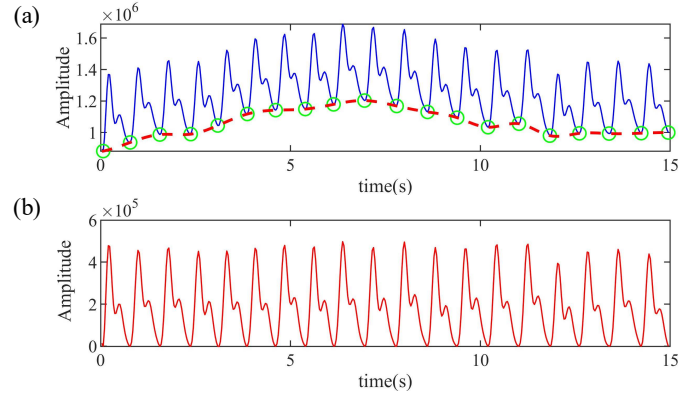


Fig. 4. Process of the FSW algorithm. (a) Baseline fitted with cubic spline interpolation: green circle is the valleys and red dotted line is the baseline, (b) PPG signal baseline removal.

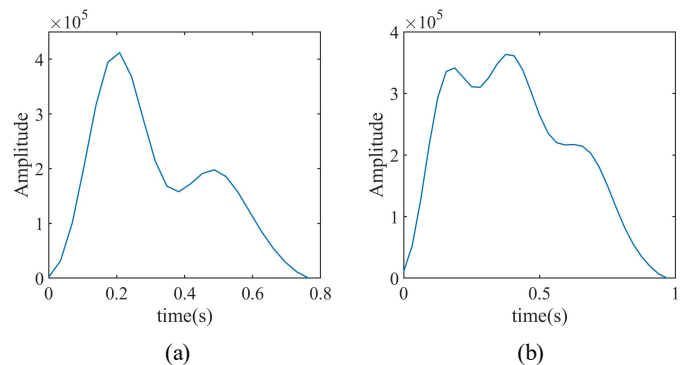


Fig. 5. Single period sample after executing FSW algorithm. (a) Single period valid sample, (b) Single period invalid sample.

signals. No obvious distortion is introduced to the signals after baseline drift removal, as shown in Fig. 4(b).

The signal is then divided into single periods. The waveform of single-period PPG signals might vary slightly for different people, but they are similar in terms of characteristics. After FSW algorithm implementation, certain parts of the damaged single-period signal might be incorrectly identified. As a result, a segmented single-period signal may comprise the falling branch of the previous signal or the rising branch of the following signal, which is usually wider than a normal signal and apparently invalid as shown in Fig. 5(b).

#### D. Feature Extraction based on Gaussian Fitting

Waveform fitting has become a promising approach on contour analysis. It breaks down different waveforms into several different sub-waves [22], [23]. Gaussian function has been used to fit ear and finger PPG pulses [24]. Both researches demonstrate the rationality and effectiveness of fitting for analyzing waveform profiles. However, these studies were more concerned with the peak timing information of the curve and the calculation of the cardiovascular index based on the sub-waves. The physiological relevance of other characteristic features, including the half-width and the peak amplitude of the modeled Gaussian curves, is very less investigated. Therefore, we propose in this study to fit the PPG signals by Gaussian function to determine the characteristic parameters

from the decomposed sub-waves, and then compare the morphological differences between PPG signals at the three blood glucose levels by statistical methods, inferring the correlation relationship between PPG signals and blood glucose. We categorize the single-period samples obtained in section III.C according to the blood glucose level divisions in Table I, and randomly select 200 samples in each group for subsequent analysis. Each PPG sample is then normalized in both amplitude (0-1) and width (50 sampling points).

Two positive Gaussian functions ( $f_1^*(n)$  and  $f_2^*(n)$ ) are applied to each normalized PPG sample  $f(n)$  ( $n = 1, 2, 3, \dots, 50$ ). They are defined as follows:

$$f_k^*(n) = H_k \times \exp\left(-\frac{2(n - n_k)^2}{W_k^2}\right) \quad (3)$$

where  $H_k$  denotes the peak amplitude,  $n_k$  represents the peak position and  $W_k$  denotes the half-width of each Gaussian curve.  $k = 1, 2$ .

Fig. 6 demonstrates the Gaussian fitting for PPG waveforms at different blood glucose levels from normal (A1 and A2), borderline (B1 and B2) and warning (C1 and C2). Six characteristic parameters from the two modeled Gaussian functions are also marked.

The least squares error (LSE) is used to assess the Gaussian fitting which is calculated by

$$LSE = \sum_{n=1}^{30} \frac{[f_1^*(n) + f_2^*(n) - f(n)]^2}{f^2(n)} \times 100\% \quad (4)$$

Therefore it is evident that the smaller the fitting errors, the smaller are the parameter errors. The parameter optimization will not be stopped until the LSE is smaller than 1.5%, which is accurate enough for waveform matching.

Table IV presents the comparison of six Gaussian features at different blood glucose levels. The peak amplitude and peak position of the first Gaussian curve have significant differences (both  $P < 0.05$ ), while the change in half-width is not obvious ( $P = 0.3$ ). At the same time, as the blood glucose level increases, the peak amplitude appears a downward trend while the peak position moves forward. The PPG waveform is traditionally considered to contain both forward and backward components [25], [26]. The forward component is derived from the ejection of the left ventricle and is more likely to be related to the first Gaussian curve. In hyperglycemia, the blood is more viscous, the peripheral resistance of the heart is higher and the peak amplitude is slightly lower than that of normal people. We also observe that the peak amplitude, peak position and half-width of the second Gaussian curve are significantly different (all  $P < 0.05$ ). At the same time, as the blood glucose level increases, the peak amplitude gradually increases, the peak position moves forward and the half-width presents an increasing trend. The backward component may be related to the second Gaussian function, which may be caused by blood circulation from the peripheral circulation system. Due to the increase of blood flow resistance, the waveform will slow down in the process of blood flow to the heart, the waveform position is relatively high and the descending branch is gentle.

Based on the comparison of the six Gaussian characteristic parameters mentioned above, we extracted a total of 28 features in the time and frequency domains. Detailed feature definitions are shown in Table V.  $H_1$ ,  $H_2$ ,  $n_1$ ,  $n_2$ ,  $W_1$ , and  $W_2$  are considered as features because they can visually show the difference among the three groups of data. In addition, other feature points can be determined by two Gaussian curves. For example, *highest\_peak* represents the maximum amplitude of the signal, actually the peak position where the first Gaussian curve appears, determined by  $n_1$ . By Gaussian fitting, we conclude that different blood glucose levels will affect the slope and amplitude of the ascending and descending branches. Therefore, *highest\_peak*, *dis\_peak* and *notch* are used to represent the height characteristics of the waveform feature points.  $n_1$ ,  $n_2$ , *time\_notch*, *timediff\_peak\_notch*, *timediff\_notch\_diastolicpeak* and *timediff\_diastolicpeak\_end* together indicate changes in blood flow rate due to blood viscosity. The *slop\_rise*, *slop\_fall*, and *slop\_peak\_diastolic* are used to describe the slope of ascending and descending branches. *area\_single*, *area\_start\_max*, *area\_max\_notch*, *area\_notch\_diastolicpeak* and *area\_diastolicpeak\_end* reflect the difference in amplitude and time more intuitively. The *width\_period* is an important feature for similar periodic signals, especially in distinguishing between valid signals and invalid ones. The extraction of the above features does not require complicated calculations and is therefore time-efficient. All these features will be used without exception for subsequent classifier training to identify invalid samples and to classify blood glucose levels.

## IV. EXPERIMENT

### A. Dataset

The research protocol was approved by the Medical Ethics Committee of Qilu Hospital of Shandong University with approval code 2019-083. The dataset was collected from 80 subjects (37.5% normal, 62.5% hyperglycemic) who were informed about the data collection procedure and signed an informed consent form. All patients have a history of more than one year without complications and confirm that they have not participated in any other ‘clinical trial’ within the previous three months. Subjects were asked to sit for three minutes to adjust their breathing and sitting position in order to reduce the impact of noise, and researchers recorded their height and weight measurements, as well as their age and medical history. The physical characteristics of the participants are listed in Table VI. Since the PPG signal is very sensitive to temperature and ambient light, data collection was undertaken in a quiet, temperature-controlled ( $24 \pm 2^\circ\text{C}$ ) and no strong light laboratory. All the subjects were uniquely numbered based on the measured blood glucose values, with individual numbers 1-30 in the G1 group, 31-58 in the G2 group, and 59-80 in the G3 group.

### B. Analysis and Diagnosis

In our experiment, single-period samples acquired from FSW algorithm contain both valid samples and invalid ones.

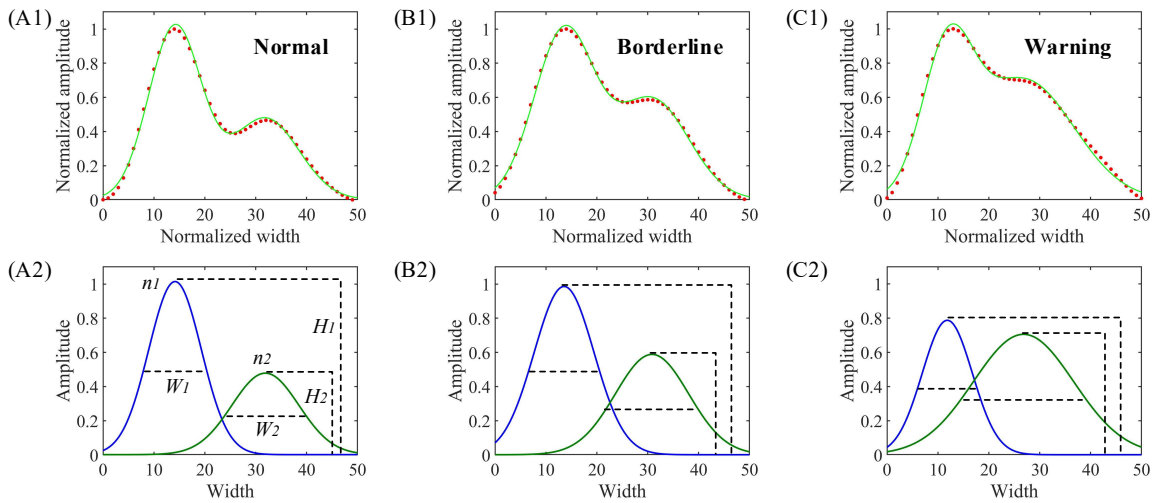


Fig. 6. Demonstration of Gaussian fitting for PPG waveforms: the normalized single period PPG signal  $f(n)$  (red scatter) and the Gaussian fitting result (solid green line) from normal (A1), borderline (B1), and warning (C1) are shown in the upper panels. The two corresponding Gaussian functions  $f_1^*(n)$  and  $f_2^*(n)$  are shown in the bottom panels. The Gaussian features: peak amplitude:  $H_1$ ,  $H_2$ , peak position:  $n_1$ ,  $n_2$  and half-width:  $W_1$ ,  $W_2$  are also shown.

TABLE IV  
COMPARISON OF SIX GAUSSIAN FEATURES AT DIFFERENT BLOOD GLUCOSE LEVELS.

Variables		Normal	Borderline	Warning	P-Value
Peak amplitude	$H_1$	$0.93 \pm 0.05$	$0.87 \pm 0.11$	$0.76 \pm 0.10$	< 0.05
	$H_2$	$0.47 \pm 0.13$	$0.61 \pm 0.07$	$0.69 \pm 0.14$	< 0.05
Peak position	$n_1$	$15.4 \pm 2.1$	$13.7 \pm 1.5$	$11.6 \pm 2.7$	< 0.05
	$n_2$	$33.1 \pm 2.7$	$31.5 \pm 1.4$	$28.2 \pm 2.6$	< 0.05
half-width	$W_1$	$14.7 \pm 1.5$	$15.4 \pm 3.2$	$15.8 \pm 2.6$	0.3
	$W_2$	$15.1 \pm 1.6$	$17.5 \pm 2.1$	$22.5 \pm 3.3$	< 0.05

Note: Data are presented as mean  $\pm$  standard deviation (SD). P-value obtained from ANOVA analysis measures the differences between the three groups categorized by blood glucose. Statistical significance is set a priori at  $P < 0.05$ .

In order to improve the blood glucose classification accuracy, invalid samples should be identified and eliminated by binary classification. The Gaussian Support Vector Machine (GSVM), Bagged Trees (BT) and K-nearest neighbor (KNN) classifiers were trained with 122 invalid samples and 140 valid samples from individuals numbered 1-15, 31-44, and 59-69. The above classifiers were tested with 114 invalid samples and 130 valid samples from the remaining individuals numbered 16-30, 45-58, and 70-80. The testing accuracy of the three classifiers was 97.54%, 96.31% and 90.57%, respectively, as shown in Table VII. A total of 6264 samples from 80 subjects were fed as input of the GSVM model. 476 samples identified as invalid ones were subsequently removed, and the remaining 5788 valid samples were adopted for subsequent analysis.

2,930 samples (from individuals 1-15, 31-44, 59-69) were used to train GSVM, BT and KNN classifiers. The labels of the training samples were set to be -1, 0 and 1, representing the G1, G2 and G3 blood glucose groups, respectively. Five-fold cross-validation was used in the experiment to reduce the impact of sample partitioning. The implementation result is

listed in table VIII. The test accuracy of 2858 samples from the remaining 40 individuals are 81.49%, 74% and 71.27%, respectively. It indicates that GSVM has the best effect for PPG signal classification.

In the subsequent analysis, we used a GSVM-based classifi-

cation model as shown in Eq. (5). The value  $C$  is the predicted class of GSVM. The coding matrix  $M$  represents the coding relationship between each binary SVM model  $f(x) = w^T x + b$  and various classes of signals in the corresponding data set. Its matrix element is  $m_{kl}$ , where  $l$  represents a binary SVM and  $k$  represents a data set category.  $g$  is the loss of decoding scheme.  $m_l$  is the predicted score of the SVM  $l$  whose prediction result is chosen according to  $m_{kl}$  [27].

$$C = \operatorname{argmin} \frac{\sum_{l=1}^L |m_{kl}| g(m_{kl}, s_l)}{\sum_{l=1}^L |m_k|} \quad (5)$$

$$M = \begin{bmatrix} 1 & -1 & 0 \\ 1 & 0 & -1 \\ 0 & 1 & -1 \end{bmatrix}$$

The Gaussian kernel function of the SVM is presented in Eq. (6), which maps finite-dimensional data to high-dimensional space. The  $\|x - x'\|$  is the square Euclidean distance between two vectors.  $\sigma$  is a free parameter that controls the radial range of action, where our  $\sigma$  is set to 0.05.

$$k(x, x') = e^{-\frac{\|x-x'\|^2}{2\sigma^2}} \quad (6)$$

$$P(i) = \begin{cases} -1 & n_{1,i} > n_{2,i}, n_{3,i} \\ 0 & n_{2,i} > n_{1,i}, n_{3,i} \\ 1 & n_{3,i} > n_{1,i}, n_{2,i} \end{cases} \quad (7)$$

TABLE V  
DEFINITIONS OF FEATURES.

Feature	Definition
$H_1$	The peak of the first Gaussian curve
$H_2$	The peak of the second Gaussian curve
$n_1$	The value of time when the amplitude is maximum
$n_2$	The value of time when diastolic occurs
$W_1$	The half-width of the first Gaussian curve
$W_2$	The half-width of the second Gaussian curve
highest_peak	Maximum amplitude of the signal
dis_peak	The amplitude of diastolic peak
notch	The amplitude of the notch
time_notch	The value of time when notch occurs
width_period	Time taken for one period
slop_rise	Rising rate of the single period from start to the peak
slop_fall	Falling rate of the single period from peak to the end
slop_peak_diastolic	Falling rate from peak to the diastolic peak
timediff_peak_notch	Total time it takes from peak to the notch
timediff_notch_diastolicpeak	Total time it takes from notch to the diastolic peak
timediff_diastolicpeak_end	Total time it takes from diastolic peak to the end
area_single	Area of the single period
area_start_max	Area from start to the peak
area_max_notch	Area from peak to the notch
area_notch_diastolicpeak	Area from notch to the diastolic peak
area_diastolicpeak_end	Area from diastolic peak to the end

TABLE VI  
PARTICIPANTS PHYSICAL CHARACTERISTICS.

Measurement	Max	Min	Mean	Std.Deviation
Age (years)	65	37	47.61	5.79
Weight (kg)	86.7	58.5	64.87	10.58
Height (m)	1.9	1.55	1.712	0.14
BMI (kg/m <sup>2</sup> )	27.36	17.58	23.56	4.45
Glucose (mmol/L)	11	3.9	7.86	2.16

In the actual clinical diagnosis, the value of the diagnosis result  $P(i)$  is -1, 0 or 1, which indicates that the blood glucose level is normal, borderline and warning respectively. In Eq. (7),  $n_{1,i}$ ,  $n_{2,i}$  and  $n_{3,i}$  represent the normal, borderline and warning blood glucose level samples of user  $i$ . When the number of samples of a certain blood glucose level is greater than the number of samples of the other two types, the user is judged to be at the blood glucose level.

Testing was implemented by those subjects numbered 16-30, 45-58 and 70-80, who did not participate in the classification model training. Each subject recorded a 60-second video by our smartphone program, which was then automatically uploaded to the cloud (PC workstation with 3.70-GHz CPU, 1080Ti GPU and 64-GB RAM) via wireless communication for PPG signal extraction, signal processing and classification. The classification results, as summarized in Table IX, were returned to the user smartphone. All single-period samples

from one subject were fed into the trained GSVM model. Using the extracted features, 11 of the 15 normal subjects were correctly classified, and 3 of them were mistakenly put into the borderline group. Among the 14 subjects with borderline blood glucose level, 10 were correctly identified. As for the 10 subjects with warning blood glucose level, 9 were correctly classified, offering an accuracy rate of 90%. This result validates the effectiveness of the features extracted and is crucial for identifying blood glucose level of the warning status. For the purpose of prompt response, we only collected 60-second video, accordingly the average number of effective samples per individual is 64. On calculating the correct probability of classification, the possibility of misdiagnosis will increase due to the small sample size. In order to provide users with a more reliable reference, three consecutive measurements are recommended. If three consecutive measurements fall into the same category, then we can reasonably believe the evaluation results. Once the three evaluation results are not the same, however, then the user is recommended to perform an invasive blood glucose meter test.

## V. CONCLUSION

This work introduces a non-invasive blood glucose monitoring system based on smartphone PPG signals and machine learning algorithms. It builds up a good basis for real-time monitoring of human physiological parameters in the home environment. Firstly, a left-hand index finger video is recorded using a smartphone and PPG signals are extracted from the video. After that the FSW algorithm removes baseline drift and divides the pre-processed signals into single periods. The result of the segmented PPG signals demonstrates the effectiveness of the developed FSW algorithm. Secondly, Gaussian fitting method is used to extract 28 features of each single-period signal in time domain and frequency domain. Finally, the blood glucose is classified as normal, borderline or warning level by a machine learning classifier with the accuracy of 81.49%, which means that the 28 features extracted are effective in separating samples of different blood glucose levels.

One of our future works is to divide the blood glucose range into more intervals to offer more precise feedbacks to the users. Therefore the PPG signal data will be augmented using Generative Adversarial Networks (GAN) to satisfy the input requirement of deep learning networks. We also wish to find more feasible features for more exact blood glucose detection. For instance, according to the hemodynamics theory, there will be energy changes in the blood during the flow, which is particularly prominent at different blood glucose levels. Therefore, Kaiser-Teager Energy feature, Spectral Entropy feature and Spectral Energy Logarithmic feature are under consideration for possible involvement. In addition, we will consider the correlation between the features to eliminate redundant features especially for real time response.

## REFERENCES

- [1] S. Ramasahayam, L. Arora, S. R. Chowdhury, and M. Anumukonda, "Fpga based system for blood glucose sensing using photoplethysmography and online motion artifact correction using adaline," *2015 9th International Conference on Sensing Technology (ICST)*, pp. 22–27, Dec 2015.

TABLE VII  
THE RESULTS OF INVALID SAMPLE CLASSIFICATION.

Classifier	Precision	Sensitivity	Specificity	F <sub>1</sub> Score	Accuracy
GSVM	96.97%	98.46%	96.49%	97.71%	97.54%
BT	95.49%	97.69%	94.74%	96.58%	96.31%
KNN	89.05%	93.85%	86.84%	91.39%	90.57%

TABLE VIII  
THE RESULTS OF BLOOD GLUCOSE LEVEL CLASSIFICATION.

Classifier	Precision	Sensitivity	Specificity	F <sub>1</sub> Score	Accuracy
GSVM	80.84%	79.58%	83.19%	80.2%	81.49%
BT	73.05%	71.05%	76.64%	72.03%	74%
KNN	69.23%	70.3%	72.14%	69.76%	71.27%

TABLE IX  
THE PREDICTION RESULTS OF GSVM.

GSVM	True level		
	Normal	Borderline	Warning
Prediction level	Normal	11	1
	Borderline	3	10
	Warning	1	9
Accuracy		73.33%	71.43%
		90.00%	

- [2] S. A. Siddiqui, Y. Zhang, J. Lloret, H. Song, and Z. Obradovic, "Pain-free blood glucose monitoring using wearable sensors: Recent advancements and future prospects," *IEEE Reviews in Biomedical Engineering*, vol. 11, pp. 21–35, 2018.
- [3] S. Sinchai, P. Kainan, P. Wardkein, and J. Koseeyaporn, "A photoplethysmographic signal isolated from an additive motion artifact by frequency translation," *IEEE Transactions on Biomedical Circuits and Systems*, vol. 12, no. 4, pp. 904–917, Aug 2018.
- [4] P. P. Pai, P. K. Sanki, S. K. Sahoo, A. De, S. Bhattacharya, and S. Banerjee, "Cloud computing-based non-invasive glucose monitoring for diabetic care," *IEEE Transactions on Circuits and Systems I: Regular Papers*, vol. 65, no. 2, pp. 663–676, Feb 2018.
- [5] S. Lekha and S. M., "Real-time non-invasive detection and classification of diabetes using modified convolution neural network," *IEEE Journal of Biomedical and Health Informatics*, vol. 22, no. 5, pp. 1630–1636, Sep. 2018.
- [6] J. Harvey, S. M. A. Salehizadeh, Y. Mendelson, and K. H. Chon, "Oxima: A frequency-domain approach to address motion artifacts in photoplethysmograms for improved estimation of arterial oxygen saturation and pulse rate," *IEEE Transactions on Biomedical Engineering*, vol. 66, no. 2, pp. 311–318, Feb 2019.
- [7] S. A. Siddiqui, Y. Zhang, Z. Feng, and A. Kos, "A pulse rate estimation algorithm using ppg and smartphone camera," *Journal of Medical Systems*, vol. 40, no. 5, pp. 1–6, May 2016.
- [8] M. Boloursaz Mashhadie, E. Asadi, M. Eskandari, S. Kiani, and F. Marvasti, "Heart rate tracking using wrist-type photoplethysmographic (ppg) signals during physical exercise with simultaneous accelerometry," *IEEE Signal Processing Letters*, vol. 23, no. 2, pp. 227–231, Feb 2016.
- [9] K. T. Tanweer, S. R. Hasan, and A. M. Kamboh, "Motion artifact reduction from ppg signals during intense exercise using filtered x-lms," *2017 IEEE International Symposium on Circuits and Systems (ISCAS)*, pp. 1–4, May 2017.
- [10] R. Raj, J. Selvakumar, and V. Maik, "Afodss: Heart rate estimation method from photoplethysmographic signals with motion artifacts using fourier-sparse dual optimization," *IEEE Sensors Journal*, vol. 19, no. 21, pp. 9953–9963, Nov 2019.
- [11] P. M. Nabeel, S. Karthik, J. Joseph, and M. Sivaprakasam, "Arterial blood pressure estimation from local pulse wave velocity using dual-element photoplethysmograph probe," *IEEE Transactions on Instrumentation and Measurement*, vol. 67, no. 6, pp. 1399–1408, June 2018.

- [12] M. A. Motin, C. K. Karmakar, and M. Palaniswami, "Ensemble empirical mode decomposition with principal component analysis: A novel approach for extracting respiratory rate and heart rate from photoplethysmographic signal," *IEEE Journal of Biomedical and Health Informatics*, vol. 22, no. 3, pp. 766–774, May 2018.
- [13] A. Hernando, M. D. Peláez, M. T. Lozano, M. Aiger, E. Gil, and J. Lázaro, "Finger and forehead ppg signal comparison for respiratory rate estimation based on pulse amplitude variability," *2017 25th European Signal Processing Conference (EUSIPCO)*, pp. 2076–2080, Aug 2017.
- [14] C. Tsai, C. Li, R. W. Lam, C. Li, and S. Ho, "Diabetes care in motion: Blood glucose estimation using wearable devices," *IEEE Consumer Electronics Magazine*, vol. 9, no. 1, pp. 30–34, Jan 2020.
- [15] E. Monte-Moreno, "Non-invasive estimate of blood glucose and blood pressure from a photoplethysmograph by means of machine learning techniques," *Artificial Intelligence in Medicine*, vol. 53, no. 2, pp. 127 – 138, 2011.
- [16] A. Hina, H. Nadeem, and W. Saadeh, "A single led photoplethysmography-based noninvasive glucose monitoring prototype system," *2019 IEEE International Symposium on Circuits and Systems (ISCAS)*, pp. 1–5, May 2019.
- [17] V. P. Rachim and W.-Y. Chung, "Wearable-band type visible-near infrared optical biosensor for non-invasive blood glucose monitoring," *Sensors and Actuators B: Chemical*, vol. 286, pp. 173 – 180, 2019.
- [18] F. Lamonaca, Y. Kurylyak, D. Grimaldi, and V. Spagnuolo, "Reliable pulse rate evaluation by smartphone," *2012 IEEE International Symposium on Medical Measurements and Applications Proceedings*, pp. 1–4, May 2012.
- [19] J. Dey, A. Gaurav, and V. N. Tiwari, "Instabp: Cuff-less blood pressure monitoring on smartphone using single ppg sensor," *2018 40th Annual International Conference of the IEEE Engineering in Medicine and Biology Society (EMBC)*, pp. 5002–5005, July 2018.
- [20] A. Sološenko, A. Petrénas, and V. Marozas, "Photoplethysmography-based method for automatic detection of premature ventricular contractions," *IEEE Transactions on Biomedical Circuits and Systems*, vol. 9, no. 5, pp. 662–669, Oct 2015.
- [21] H. Wang, X. Wang, J. R. Deller, and J. Fu, "Shape-preserving preprocessing for human pulse signals based on adaptive parameter determination," *IEEE Transactions on Biomedical Circuits and Systems*, vol. 8, no. 4, pp. 594–604, Aug 2014.
- [22] S. C. Millasseau, J. M. Ritter, K. Takazawa, and P. J. Chowienczyk, "Contour analysis of the photoplethysmographic pulse measured at the finger," *IEEE Transactions on Instrumentation and Measurement*, vol. 24, pp. 1449–1456, Aug. 2006.
- [23] D. Jang, S. Park, and M. Hahn, "A gaussian model-based probabilistic approach for pulse transit time estimation," *IEEE Journal of Biomedical and Health Informatics*, vol. 20, no. 1, pp. 128–134, Jan 2016.
- [24] U. Rubins, "Finger and ear photoplethysmogram waveform analysis by fitting with gaussians," *Medical & Biological Engineering & Computing*, vol. 46, no. 12, pp. 1271–1276, Dec 2008.
- [25] K. Soerensen, A. K. Verma, A. Blaber, J. Zanetti, S. E. Schmidt, J. J. Struijk, and K. Tavakolian, "Challenges in using seismocardiography for blood pressure monitoring," *2017 IEEE Computing in Cardiology (CinC)*, pp. 1–4, Sep. 2017.

- [26] H. Wu, C. Lee, A. Liu, W. Chung, C. Tang, C. Sun, and H. Yip, "Arterial stiffness using radial arterial waveforms measured at the wrist as an indicator of diabetic control in the elderly," *IEEE Transactions on Biomedical Engineering*, vol. 58, no. 2, pp. 243–252, Feb 2011.
- [27] I. Steinwart, D. Hush, and C. Scovel, "An explicit description of the reproducing kernel hilbert spaces of gaussian rbf kernels," *IEEE Transactions on Information Theory*, vol. 52, no. 10, pp. 4635–4643, Oct 2006.



**Gaobo Zhang** was born in Yantai, China. He received the B.S. degree from Henan University of Technology, Zhengzhou, China, in 2013.

Currently, he is with the College of Electronic and Information Engineering, Southwest University, China, and also with the Shandong Provincial Key Laboratory of Network Based Intelligent Computing as a graduate student. His research interests include wearable sensing technology and biomedical signal processing.



**Benny Lo** (SM'16) received the B.A.Sc. degree in electrical engineering from the University of British Columbia, Canada, the M.Sc. (distinction) degree in electronics from King's College London, U.K., and the Ph.D. degree in computing from Imperial College London, U.K. in 1995, 2000, and 2007 respectively. He is currently a Senior Lecturer with the Hamlyn Centre and the Department of Surgery and Cancer, Imperial College London. As one of the pioneers in body sensor networks (BSN), he has introduced numerous new platform technologies and

novel approaches for wellbeing, and healthcare applications. His research interests include computer vision, machine learning, BSN, microelectronics, and wearable technologies for healthcare and wellbeing. He is an Associate Editor of the IEEE Journal of Biomedical Health Informatics, and he also served as the Chair of the IEEE Engineering in Medicine and Biology Society (EMBS) Wearable Biomedical Sensors and Systems Technical Committee (2018-19).



**Zhen Mei** received the Ph.D. degree in Colloid and Interface Chemistry from Shandong University, China, in 2011. She is currently a lecturer with the College of Chemistry and Chemical Engineering, Southwest University, China. Dr. Mei's research interests include synthesis of nanomaterials and their application in biomedical, chemical sensor, etc. As the first author or corresponding author she has published more than 10 papers and patents in international journals and conference proceedings.



**Dongyi Chen** is currently a professor at the University of Electronic Science and Technology China. He received his doctorate degree from Chongqing University in 1997. In 1998, he worked at the University of Toronto as a visiting scientist. From 2002 to 2005, he worked as visiting professor with at GVU of Georgia Institute of Technology. In 2009, he began to cooperate with TZI (Technologie-Zentrum Informatik und Informationstechnik) of University of Bremen, Germany and was a co-doctoral mentor. He was member of ISWC (International Semantic

Web Conference) 2010 Technical Committee, and he is co-chair of IEEE SMCS (Systems, Man, and Cybernetics Society) TC on Interactive and Wearable Computing and Devices. He organized or guided China Wearable Computing Conference as general chair, executive chair or leader of the steering committee of the conference.



**Yuan Zhang** (SM'14) received the M.S. degree in communication systems and the Ph.D. degree in control theory and engineering both from Shandong University, China, in 2003 and 2012, respectively. He is currently a Professor with the College of Electronic Information Engineering, Southwest University, China. Dr. Zhang was a visiting professor with the Computer Science Department, Georgia State University, USA, in 2014. Dr. Zhang's research interests include wearable sensing for smart health, machine learning for auxiliary diagnosis, and biomedical big data analytics. He is a member of IEEE EMBS Wearable Biomedical Sensors and Systems Technical Committee. He is an associate editor for IEEE Reviews in Biomedical Engineering, IEEE Open Journal of Engineering in Medicine and Biology and IEEE Access. He has served as Leading Guest Editor for six special issues of IEEE, Elsevier, Springer and InderScience publications. He has served on the technical program committee for numerous international conferences. Dr. Zhang is a Senior Member of ACM.



**Yuanting Zhang** (Fellow, IEEE) received the B.S. and M.S. degrees in telecommunication from the Department of Electronics, Shandong University, China, in 1976 and 1981, respectively, and the Ph.D. degree in electrical engineering from the University of New Brunswick, Canada, in 1990. He is the first Head of Division of Biomedical Engineering and Professor of the Department of Electronic Engineering at the Chinese University of Hong Kong (CUHK), Hong Kong. He serves concurrently as the Director of the Key Lab of Health Informatics of the Chinese Academy of Sciences (HICAS), and the founding Director of the CAS-SIAT (Shenzhen Institutes of Advanced Technology, Chinese Academy of Sciences) Institute of Biomedical and Health Engineering. His research interests include wearable medical devices, body sensor networks, neural engineering, etc. Dr. Zhang was previously the Vice-President of the IEEE-EMBS in 2000–2001. He is currently the Editor-in-Chief of the IEEE Reviews in Biomedical Engineering, and was the Editor-in- Chief for IEEE Transactions on Information Technology in Biomedicine and the founding Editor-in-Chief of IEEE Journal of Biomedical and Health Informatics. He is a Fellow of the International Academy of Medical and Biological Engineering and the American Institute of Medical and Biological Engineering.



**Xuesheng Ma** received the M.S. degree in integrated Chinese Medicine Conventional Medicine in Geriatrics Disease, Shandong University of Traditional Chinese Medicine, China, in 2000. He is a Senior Lecturer with School of Natural Medicine in University of the Western Cape, Cape Town, South Africa. His research mainly focuses on Type 2 Diabetes Mellitus diagnose and management in conventional medicine and Chinese Medicine. He is a council member of World Federation of Chinese Medicine Societies. He participated in China-South Africa joint project entitled "Research on anti-diabetic South Africa indigenous screening and their anti-diabetic molecular mechanism investigation", with fruitful research outcomes presented in several publications.